Neuroscience Research 191 (2023) 28–37

Contents lists available at ScienceDirect

Neuroscience Research

journal homepage: www.sciencedirect.com/journal/neuroscience-research

Alternative strategy for driving voltage-oscillator in neocortex of rats

Takako Fukuda [a], Takashi Tominaga [b], Yoko Tominaga [b], Hiroyuki Kanayama [a,c], Nobuo Kato [d], Hiroshi Yoshimura [a,*]

[a] Department of Molecular Oral Physiology, Institute of Biomedical Sciences, Tokushima University Graduate School, Kuramoto, Tokushima 770-8504, Japan
[b] Institute of Neuroscience, Tokushima Bunri University, Shido, Kagawa 769-2123, Japan
[c] Department of Oral and Maxillofacial Surgery, National Hospital Organization Osaka National Hospital, Osaka 540-0006, Japan
[d] Department of Physiology, Kanazawa Medical University, Uchinada-cho, Ishikawa 920-0293, Japan

ARTICLE INFO

Keywords:
Visual cortex
Oscillation
Voltage-oscillator
Caffeine
Optical recording
Signal propagation

ABSTRACT

Information integration in the brain requires functional connectivity between local neural networks. Here, we investigated the interregional coupling mechanism from the viewpoint of oscillations using optical recording methods. Low-frequency electrical stimulation of rat neocortical slices in a caffeine-containing medium induced oscillatory activity between the primary visual cortex (Oc1) and medial secondary visual cortex (Oc2M), in which the oscillation generator was located in the Oc2M and was triggered by a feedforward signal. During to-and-fro oscillatory activity, neural excitation was marked in layer II/III. When the upper layer was disrupted between Oc1 and Oc2M, feedforward signals could propagate through the deep layer and switch on the oscillator in the Oc2M. When the lower layer was disrupted between Oc1 and Oc2M, feedforward signals could propagate through the upper layer and switch on the oscillator in the Oc2M. In the backward direction, neither the upper layer cut nor the lower layer cut disrupted the propagation of the oscillations. In all cases, the horizontal and vertical pathways were used as needed. Fluctuations in the oscillatory waveforms of the local field potential at the upper and lower layers in the Oc2M were reversed, suggesting that the oscillation originated between the two layers. Thus, the neocortex may work as a safety device for interregional communications in an alternative way to drive voltage oscillators in the neocortex.

1. Introduction

Voltage oscillations in cortical neurons are a well-known phenomenon. These oscillations are composed of repetitive membrane potential fluctuations. When multiple neurons are activated synchronously, rhythmic waves emerge. It is widely accepted that an adequate activity balance between excitatory and inhibitory neural networks is required to produce rhythmic waves (Lourenço et al., 2020; Sase et al., 2017; Shu et al., 2003; Melamed et al., 2008; Zhang and Zhang, 2020). These neural wave dynamics may play important roles in the brain, including information coding, integration, synaptic plasticity, and regional coupling (Buzáki and Draguhm, 2004; Buzáki and Watson, 2012; Chadwick et al., 2015; Engel et al., 2001; Ermentrout and Kleinfeld, 2001; Singer, 2018).

Individual local areas in the brain play a role in individual functions, which is called the localization of cerebral function. The execution of integrative functions requires functional connectivity between distant local network nodes (Sporns et al., 2007). Recently, several functional connections between nodes have been identified as large-scale networks (Bressler, Menon, 2010; Petersen, Sporns, 2015; Qi et al., 2018; Suo et al., 2021). The signals from various areas converge at the local network nodes, and the nodes deliver the signals to other areas. One important strategy of information integration between nodes may be oscillation with dynamic interregional coupling (Masquelier et al., 2009; Oku and Aihara, 2010). Regarding neural oscillations, the essential role of neural networks that generate oscillations is to encode information and route the coded information through multiple mechanisms (Sejnowski and Paulsen, 2006; Masquelier et al., 2009; Buzáki and Watson, 2012; Chadwick et al., 2015; Panzeri et al., 2015). The oscillations work in various regions and sizes of neural networks (Buzáki et al., 2013; Singer, 2018). However, a comprehensive understanding of this oscillation is lacking.

Cortical networks are complex, but hierarchically ordered for cortical processing (Douglas and Martin, 2004; Singer, 2021). In

* Correspondence to: Department of Molecular Oral Physiology, Institute of Biomedical Sciences, Tokushima University Graduate School, 3–18-15, Kuramoto, Tokushima 770-8504, Japan.
E-mail address: hyoshimu@tokushima-u.ac.jp (H. Yoshimura).

https://doi.org/10.1016/j.neures.2023.01.002
Received 1 November 2022; Received in revised form 11 January 2023; Accepted 11 January 2023
Available online 13 January 2023

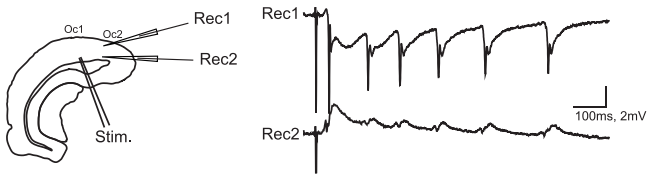

Fig. 1. Caffeine-assisted oscillation in the secondary visual cortex. Left: Illustration of a slice indicating the electrical stimulation site and recording sites of local field potentials. Right: Waveforms of the local field potential obtained from layers II/III and VI. These oscillations were induced by caffeine application to the medium. The direction of the repetitive wave fluctuation was reversed between the two oscillations.

general, the primary sensory area sends feedforward signals to a higher level of sensory area, whereas the higher area sends back signals as top-down feedback information. Thus, feedforward and feedback interactions play a core role in cortical function (Shao and Burkhalter, 1996; Johnson and Burkhalter, 1997; Singer, 2021; D'Souza et al., 2022). The visual cortex is composed of horizontal layers and vertical columns, and feedforward and feedback connections exist between the primary visual cortex (Oc1) and secondary visual cortex (Oc2). We have previously reported the dynamic behavior of oscillations in the visual cortex of rat brain slices by applying caffeine to the extracellular medium (Yoshimura et al., 2001, 2003, 2016). In caffeine-assisted oscillations, electrical stimulation is required to initiate oscillatory activities. The initial neural signal evoked by the stimulation of Oc1 travels along the upper and lower layers in parallel and triggers the neural oscillator in Oc2. The oscillator then delivers repetitive signals in a back-and-force manner (Yoshimura et al., 2001, 2003, 2016). This may be a model of the dynamic interaction between nodes via oscillation. However, the role of the neocortex as a device of interregional coupling using neural oscillation is unclear. In an attempt to clarify this question, we performed experiments using optical recording methods by applying caffeine-assisted oscillation to rat brain slices, including cortical visual areas. This mesoscopic approach may help to understand region-to-region interactions in the brain from the dynamical viewpoint of oscillation.

2. Methods

2.1. Animals and slice preparation

All experiments were approved by the Animal Care Committee of Tokushima Bunri University (KP22–83–4) and Kanazawa Medical University (2012077). Experiments were performed in accordance with the Guidelines for the Ethical Use of Animals of the Physiological Society of Japan. All efforts were made to minimize both the number of animals and their suffering.

Wistar rats (25–29 days old) were used for electrophysiological and optical recordings. Before starting these recordings, rats were decapitated under deep isoflurane anesthesia, and their brains were quickly removed and placed in cold medium (2–4 °C) containing 124 mM NaCl, 3.3 mM KCl, 1.25 mM NaH_2PO_4, 1.3 mM $MgSO_4$, 2 mM $CaCl_2$, 26 mM $NaHCO_3$, and 10 mM D-glucose that was saturated with 95% O_2-5% CO_2. Brain slices (250–300 μm thick), including the primary and secondary visual cortices, were prepared using a slicer. Once cut, slices were left at room temperature for at least 1 h before starting the recording session.

2.2. Electrophysiological and optical recordings

Slices were placed in a submerged-type chamber that was set on the stage of an upright microscope (IMT-2, Olympus, Tokyo, Japan) and perfused with medium (30 °C; 5 ml/min). A bipolar tungsten electrode for stimulation was inserted into the region between the gray and white matter (WM) in Oc1. The duration and intensity of the stimuli were 80 μs and 250–350 μA, respectively. Synaptic responses were elicited by electrical stimulation. From Oc1 and Oc2M, as described in the atlas by Paxinos and Watson (1997), we recorded the neural responses. The delineation of area borders was based on the descriptions by Swanson (1992) and Zilles in Paxinos' 'The rat nervous system' (Zilles and Wree, 1995).

Extracellular recordings were performed to observe electrophysiological responses. Micropipettes for field potential recordings were filled with 3 M NaCl and inserted into layer II/III in Oc1, Oc2M, and layer VI in Oc2M, as needed. Synaptic responses were recorded with a bridge-equipped amplifier (Axoclamp-2B; Axon Instruments, Foster City, CA, USA), digitized using an AD converter (at the rate of 2.5–5 kHz; Digidata 1200; Axon Instruments) and stored on a personal computer for offline analysis.

Optical recording methods have been used with voltage-sensitive dyes to observe the spatiotemporal dynamics of propagating neural activities. Details of the optical recording system used in this study have been described elsewhere (Tanifuji et al., 1994; Yoshimura et al., 2003; Tominaga et al., 2002). The voltage-sensitive dye NK2761 (0.125 mg/ml; Nihon Kanko, Okayama, Japan) was used for optical recordings. The camera unit of a Fujix HR Deltaron 1700 optical imaging system (Fuji Photo Film, Tokyo, Japan) contains a photodiode array of 128 × 128 elements. Using a 10 × objective lens, the entire array corresponded to a 2.24 × 2.24 mm area of tissue. A total of 16 responses elicited by the WM stimulation were averaged to form a run. Neural activity was recorded as intensity changes in transmitted light hitting each photodiode, with a temporal resolution of 0.6 msec/frame. The signal intensity was measured with 8-bit resolution and expressed as the relative, dimensionless difference from the baseline intensity, which was set as zero.

2.3. Protocol of oscillation induction

According to the purposes of the study, caffeine (3 mM) (purchased from Wako Pure Chemical Industries, Osaka, Japan) was added to the medium, and all recordings were performed in medium with 0.5 mM Mg^{2+}. We have developed a protocol in which synchronized population oscillation of synaptic potentials at a frequency of 8–10 Hz is induced in slices of the rat visual cortex and somatosensory cortex bathed in a caffeine-containing medium (Yoshimura et al., 2001, 2003, 2016). This protocol also involves a long-range signal propagation. Throughout the experiments, the same protocol was used to observe signal travel between Oc1 and Oc2M.

3. Results

We have previously reported that low-frequency electrical stimulation of Oc1 generates stable membrane potential oscillations in rat brain slices when caffeine is applied to the extracellular medium (Yoshimura et al., 2001, 2003, 2005, 2016). The summary is as follows: (1) The oscillation is composed of an early signal-propagating phase and later back-propagation phases. (2) The early phase is mainly non-NMDA receptor activity-dependent, and the later phase is NMDA receptor activity-dependent. (3) The origins of the NMDA receptor-dependent phase (oscillator) are the Oc2M and/or lateral secondary visual cortex (Oc2L). (4) The retrosplenial cortex also has an oscillator, which is switched on by neural input from Oc1.

3.1. Local field potentials in the Oc2M

In the present study, we used the same methods as described above. First, we confirmed whether stable oscillations were generated in the Oc2M. Low-frequency electrical stimulation (0.3 Hz) was delivered at

the border area between layer VI and the WM of Oc1. Low-frequency stimulation was continued for approximately 30 min. When frequency of the stimulation was changed from 0.3 Hz to 0.03 Hz, stable oscillation was induced in the Oc2M. Field potential recordings were performed in both the upper and lower layers (Fig. 1). In the upper layer, a large downward oscillatory potential was observed. In contrast, a small upward oscillatory potential is observed in the lower layer. It is important to note that the direction of the wave fluctuation was reversed between the oscillations at the upper and lower layers, which shows that, considering the electrical field in this electrophysiological phenomenon, the area of the current sink is located between the upper and lower layers. In other words, oscillations based on synaptic activity are generated between the upper and lower layers.

3.2. Upper layer cut between Oc1 and Oc2M

We then observed the dynamics of the oscillations using optical recording methods (Fig. 2A). The area of the optical recording is shown in the slice illustration (open blue rectangle). The regions of interest (ROIs) were numbered and displayed in one of the optical images. The time-course responses recorded at the respective ROIs were arranged. The presumed origin of the oscillation is Oc2M. Sequence images for every 0.6 msec showed that the initial signal propagated toward the Oc2M, in which optical signals were marked along the upper layer. After the initial signal disappeared, oscillatory signals appeared in Oc2M. For the same slice, a vertical cut from the surface to layer IV was executed in an intermediate area between Oc1 and Oc2M (Fig. 2B). The area of the optical recording was changed and is shown on the slice illustration (open blue rectangle). ROIs were numbered according to changes in the

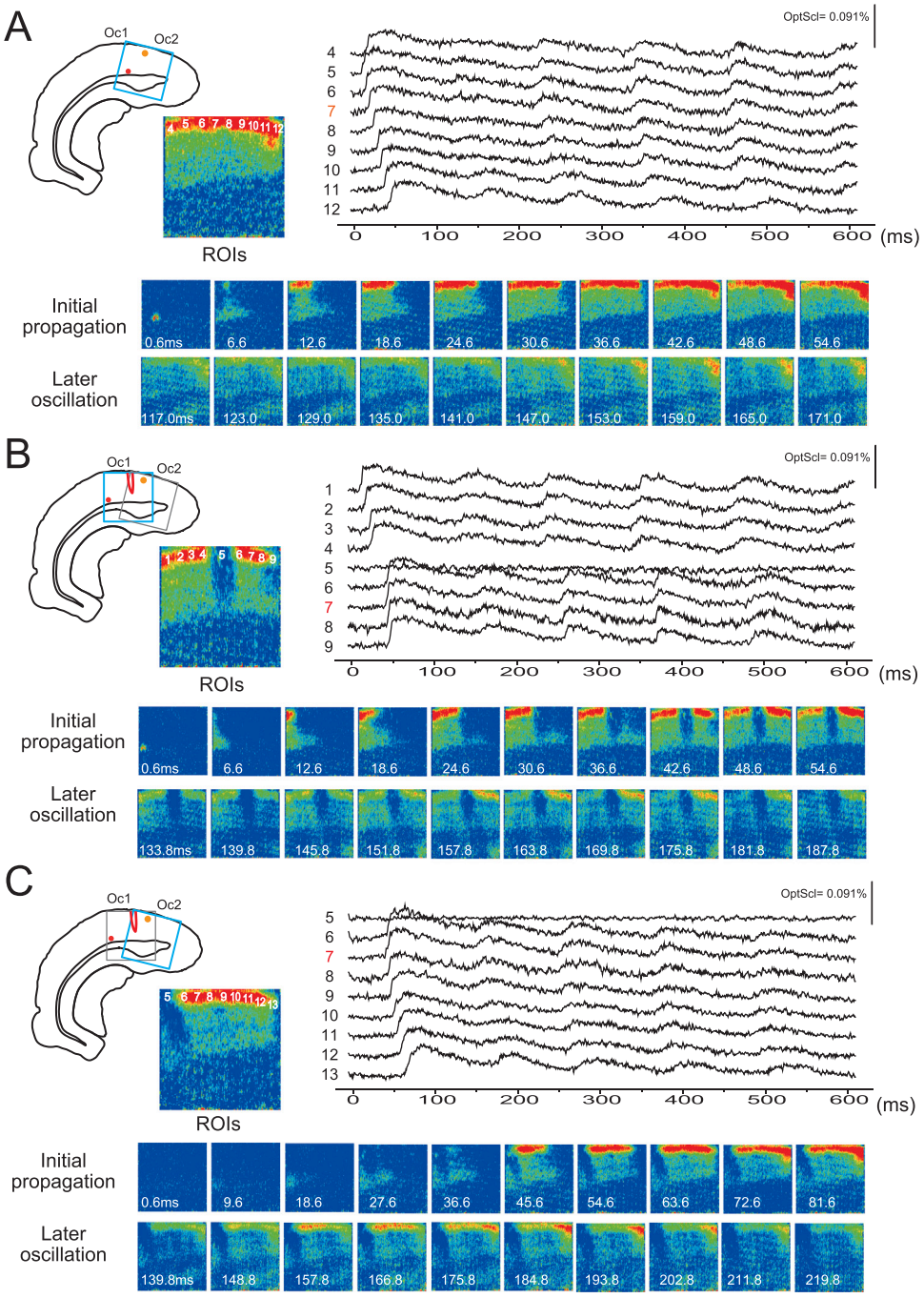

Fig. 2. Influences of disconnection at upper layer on dynamics of oscillations. (A) Upper left: Illustration of a slice indicating the electrical stimulation site (red-circle) and area (blue-rectangle) from which optical signals were recorded, and representative optical image with ROIs. Upper right: Time courses of responses at ROIs 4–12 were arranged in numerical order. Note that the presumed wave generation site of later oscillatory phase was shown as orange-circle in the illustration of a slice (ROI 7). Lower: Time-lapse optical images of signal propagation after induction of oscillations. Initial propagation component and representative later oscillation component were shown respectively. (B) Upper left: Illustration of a slice indicating the electrical stimulation site (red-circle) and area (blue-rectangle) from which optical signals were recorded, and representative optical image with ROIs. The site of vertical cut in the upper layer was shown in the slice illustration. Upper right: Time courses of responses at ROIs 1–9 were arranged in numerical order. Note that ROI 5 was below vertical cut area, and optical response at ROI 5 was disappeared. Lower: Time-lapse optical images of signal propagation after induction of oscillations. Initial propagation component and representative later oscillation component were shown respectively. (C) Optical recording area was changed. Upper left: Illustration of a slice indicating the electrical stimulation site (red-circle) and area (blue-rectangle) from which optical signals were recorded, and representative optical image with ROIs. Time courses of responses at ROIs 5–13 were arranged in numerical order. Note that ROI 5 was below vertical cut area, and optical response at ROI 5 was disappeared. Lower: Time-lapse optical images of signal propagation after induction of oscillations. Initial propagation component and representative later oscillation component were shown respectively.

recording area and are shown in one of the optical images. The time-course responses recorded at the respective ROIs were arranged. At ROI 5, the time-course responses were flat, suggesting that the initial signal propagation stopped at the area of the upper layer cut. However, marked oscillatory responses appeared in ROIs 6, 7, 8, and 9. Sequence images show that the initial signal propagated through the deep layer, and then the signal propagated in Oc2M along both the deep and upper layers. Later, an oscillatory phase appeared in the upper layer in Oc2M. Then, we changed the area of the optical recording, and the recording area is shown in the slice illustration (open blue rectangle) (Fig. 2C). This figure clearly shows that the signal propagated through the deep layer switched on the oscillator in the Oc2M. Thus, the signal input along the deep layer alone can switch on the oscillator.

3.3. Lower layer cut between the Oc1 and Oc2M

In another slice, we observed the dynamics of the same type of oscillation as shown in Fig. 2A (Fig. 3A). The presumed origin of the oscillation is Oc2M. Sequence images show that the initial signal propagates toward Oc2M, in which the optical signals are marked along the upper layer. After the initial signal disappeared, oscillatory signals appeared in Oc2M. For the same slice, a vertical cut from layer IV to the WM was made at an intermediate area between Oc1 and Oc2M (Fig. 3B). The area of the optical recording is shown in the slice illustration (open blue rectangle). The ROIs were numbered and shown in one of the optical images of the upper layer. The time-course responses recorded at the respective ROIs were arranged. Although a deep-layer cut was made, aspects of the initial signal propagation and later oscillatory events in the upper layer were almost the same as those before the cut was executed. It is necessary to confirm whether the deep areas were completely cut. The ROIs were then numbered in layer VI and are shown in the optical image (Fig. 3B bottom). The time-course responses recorded at the respective ROIs were arranged. At ROIs 2 and 3, the time-course responses were flat, suggesting that the initial signal propagation was stopped at the area of the lower layer cut. However, the initial signal propagation along the deep layer appeared from ROIs 4–9. This figure clearly shows that the signal propagated through the upper layer and switched on the oscillator in Oc2M. Thus, the signal input along the upper layer alone can switch on the oscillator.

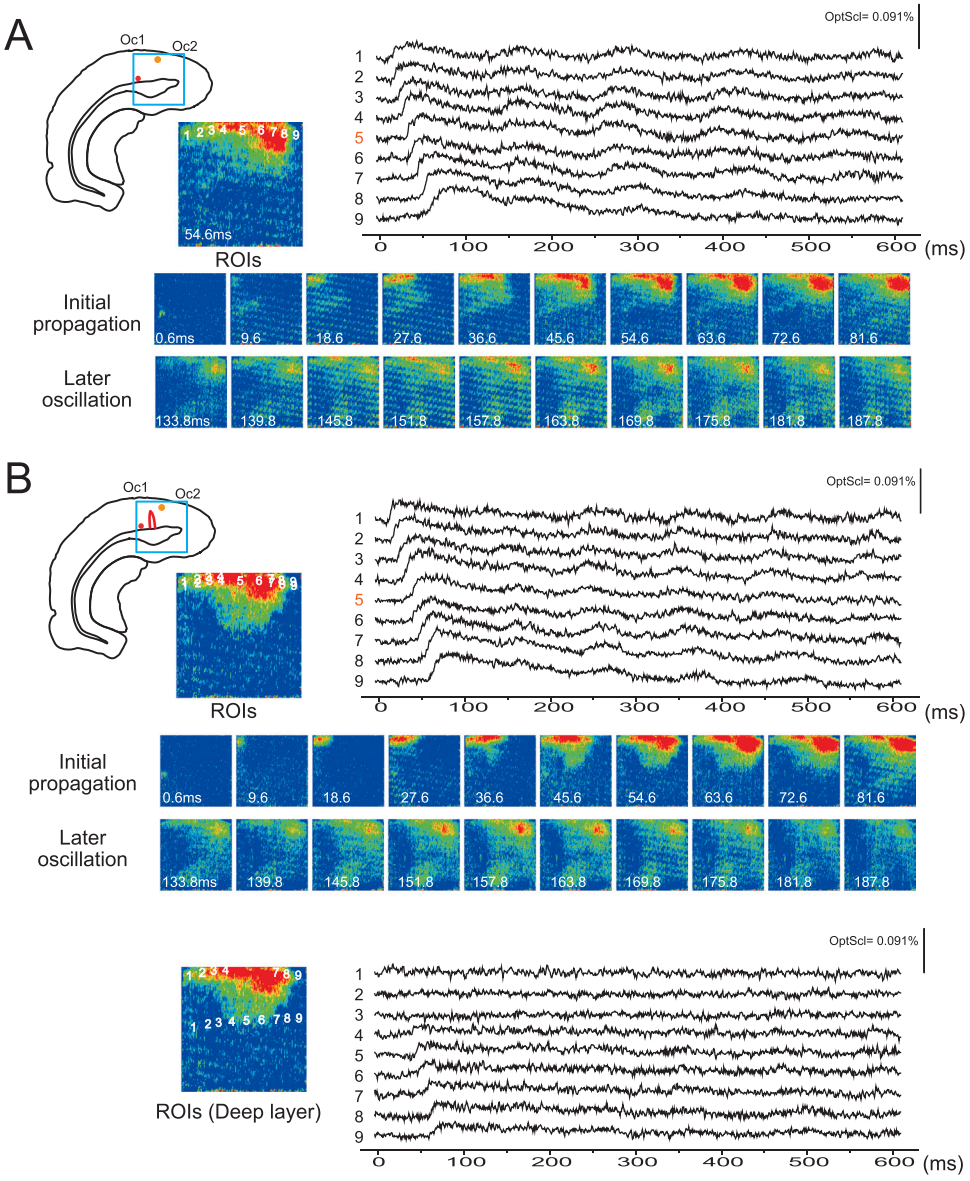

Fig. 3. Influences of disconnection at lower layer on dynamics of oscillations. (A) Upper left: Illustration of a slice indicating the electrical stimulation site (red-circle) and area (blue-rectangle) from which optical signals were recorded, and representative optical image with ROIs. Upper right: Time courses of responses at ROIs 1–9 were arranged in numerical order. Note that presumed wave generation site of later oscillatory phase was shown as orange-circle in the illustration of a slice (ROI 5). Lower: Time-lapse optical images of signal propagation after induction of oscillations. Initial propagation component and representative later oscillation component were shown respectively. (B) Upper left: Illustration of a slice indicating the electrical stimulation site (red-circle) and area (blue-rectangle) from which optical signals were recorded, and representative optical image with ROIs. The site of vertical cut in the lower layer was shown in the slice illustration. Upper right: Time courses of responses at ROIs 1–9 were arranged in numerical order. Note that ROI 3 was the area above the lower cut, and optical response at ROI 3 was not disappeared. Lower: Time-lapse optical images of signal propagation after induction of oscillations. Initial propagation component and representative later oscillation component were shown respectively. Middle: Time-lapse optical images of signal propagation after induction of oscillations. Initial propagation component and representative later oscillation component were shown respectively. Lower: Representative optical image with ROIs is shown. Time courses of responses at ROIs 1–9 along layer VI were arranged in numerical order. Note that ROI 2 and 3 were below vertical cut area, and optical response at ROIs 2 and 3 was disappeared.

3.4. Onset times of oscillatory events in the Oc2M along disconnected layer

In the case of the upper layer cut, aspects of spatio-temporal signal propagation along the upper layer show that the signal traveling from Oc1 stops in the area of disconnection, but takes a roundabout route and then restarts from the upper layer of the Oc2M side. In the case of the lower layer cut, the signal followed a roundabout route and restarted from the lower layer of the Oc2M side. In both cases, the restart signal can switch on oscillatory events in Oc2M. Then, we investigated the extent to which the disconnection delayed the onset time of the oscillatory events in Oc2M. In the case of the upper-layer cut, the time required to cross the disconnected area was prolonged along the upper-layer route, but not the lower-layer route (Fig. 4A, n = 3). In the case of the lower-layer cut, the time required to cross the disconnected area was prolonged along the lower-layer route but not the upper-layer route (Fig. 4B, n = 3). Together with these results, we found that the time required to go across the disconnected area was significantly prolonged along the disconnected layer (before cut: 7.6 ± 1.96 ms, after cut: 26.8 ± 4.47 ms, paired t-test, $p = 3.32 \times 10^{-4}$, n = 6), but not intact layer route (before cut: 8.3 ± 2.19 ms, after cut: 9.33 ± 3.23 ms, paired t-test, p = 0.38, n = 6) (Fig. 4C), in which the signal traveling by way of a roundabout route causes delay in onset time of the oscillatory events. It is important to note that disconnection in the neocortex cannot stop the signal from traveling, as long as the horizontal pathways are partially intact, with the result that the oscillator is successfully switched on the input signal.

3.5. Simultaneous recordings of local field potential from the Oc1 and Oc2

Considering these results, the oscillator equipped in the Oc2M is alternatively switched on by signals from the upper or lower layers. In addition, the vertical pathway sends a signal from the upper layer to the deep layer, and vice versa. Another important finding is that, even if the horizontal connections between Oc1 and Oc2M are incomplete, the oscillator in Oc2 can work independently.

Investigation of neural dynamics using optical recording methods revealed that major electrical activities were elicited in layer II/III between Oc1 and Oc2M. We then simultaneously performed field potential recordings from Oc1 and Oc2M. Oscillatory activity was induced using the same methods described above. First, we confirmed that the two electrodes simultaneously captured clear field potential oscillations from Oc1 and Oc2M (Fig. 5-A1). Then, for the same slice, a vertical cut from the surface to layer IV was executed at an intermediate area between Oc1 and Oc2M (Fig. 5-A2). It appears that the upper-cut manipulation has almost no effect on the oscillation dynamics, showing that the trigger signal arrived in the Oc2M through the deep area between Oc1 and Oc2M. Then, for the same slice, a vertical cut from the surface to layer VI was made at an intermediate area between Oc1 and Oc2M (Fig. 5-A3). Attenuated oscillations were confirmed at Oc1, but no response was observed at Oc2M, showing that the initial trigger signal did not arrive at the oscillator in Oc2M, and that a small oscillator was also equipped in Oc1 independently from Oc2M. Then, the stimulation electrode was moved from Oc1 to Oc2M, and the oscillator in Oc2M was triggered by electrical stimulation (Fig. 5-A4). The oscillatory dynamics were almost the same, even though the horizontal cortical pathway between Oc1 and Oc2M was disconnected, showing that the oscillator can work completely and independently from Oc1.

In subsequent experiments, we also performed field potential recordings from Oc1 and Oc2M simultaneously. Oscillatory activity was induced using the same methods described above. First, we confirmed that the two electrodes simultaneously captured clear field potential oscillations from Oc1 and Oc2M (Fig. 5-B1). Then, for the same slice, a vertical cut from layer IV to layer VI was executed at an intermediate area between Oc1 and Oc2M (Fig. 5-B2). It seems that the lower-cut manipulation has almost no effect on the oscillation dynamics, showing that the trigger signal arrived in the Oc2M through upper layer between Oc1 and Oc2M. Then, for the same slice, a vertical cut from the surface to layer VI was executed at an intermediate area between Oc1 and Oc2M (Fig. 5-B3). Attenuated oscillations were confirmed at Oc1, but no response was observed at Oc2M, showing that the initial trigger signal did not arrive at the oscillator in Oc2M, and that a small oscillator was also equipped in Oc1 independently from Oc2M. The stimulation electrode was then moved from Oc1 to Oc2M, and the oscillator in the Oc2M was triggered by electrical stimulation (Fig. 5-B4). The oscillatory dynamics were almost the same, even though the horizontal cortical pathway between Oc1 and Oc2M was disconnected, showing that the oscillator can work completely and independently from Oc1.

3.6. Influence of slice cuts on oscillation sizes in the Oc1 and Oc2M

We investigated how disruptions of horizontal pathways between Oc1 and Oc2 by three manipulations, the upper layer cut, lower layer cut, and whole layer cut, influence signal communications using the field potential recording method from several slices in the three cases. First, it appears that the upper layer cut manipulation has almost no effect on the oscillation dynamics (Fig. 5-A2). Second, it seems that lower layer cut manipulation has almost no effect on oscillation dynamics (Fig. 5-B2). Third, it seems that the whole-layer cut attenuates oscillatory dynamics in Oc1 (Fig. 5-A3, B-3), but not in Oc2M (Fig. 5-A4, B-4). We investigated whether these findings were applicable to other slices. We estimated the number of waves of oscillatory events as the oscillation size. In the case of the upper layer cut, there was no significant difference in the oscillation sizes in Oc1 before and after the upper layer cut. Similarly, there was no significant difference in the oscillation sizes in Oc2M before and after the upper layer cut (Fig. 6 A, n = 14). In the case of the lower-layer cut, there was no significant difference in the oscillation sizes in Oc2M before and after the lower-layer cut. Similarly, there was no significant difference in the oscillation sizes in Oc2M before and after the lower-layer cut (Fig. 6B, n = 5). In contrast, in the case of whole-layer cut, there was a significant difference in oscillation size in Oc1 before and after the whole-layer cut (before cut: 4.5 ± 1.1, after cut: 3.0 ± 0.76, paired t-test, p = 0.0094, n = 8, Fig. 6C).

4. Discussion

Brain waves are generated by the integration of individual voltage oscillations generated in widely located local networks in the brain, in which interregional signal communications are especially important. Electrophysiological experiments using brain slice preparation are an excellent strategy for elucidating neural functions in detail. However, the mesoscopic level of network activities in slice preparation, such as interregional signal communication, are difficult to induce in normal artificial cerebrospinal fluid. In the present study, we used an extracellular medium with caffeine (3.0 mM) under a reduced Mg^{2+} concentration (0.5 mM). The medium equally increased the excitability in the local intrinsic networks and corticocortical projections included in the whole slice. Indeed, the medium is far from physiological conditions; however, from the viewpoint of interregional signal communication, our experimental protocol should be useful for eliciting hidden mechanisms in slice preparation. The effects of caffeine and reduced Mg^{2+} concentration on the dynamics of neural activity at the single neuron level as well as mesoscopic network level elicited in slice preparations have been described in detail in our previous reports (Yoshimura et al., 2001, 2003).

4.1. Feedforward and feedback components of the oscillations

A recent study reported that feedforward projections from the primary visual cortex send signals to layers II/III, V, and VI in the secondary visual cortex, whereas feedback projections from the secondary visual

cortex also send signals to layers II/III, V, and VI in the primary visual cortex. Thus, visual cortical areas have a cortico-cortical loop (Young et al., 2021). In our studies, regarding the mesoscopic dynamics of synchronized oscillations, we observed that, after the oscillator in the Oc2M and/or the Oc2L receives trigger signals from Oc1, the oscillator begins to work and delivers repetitive oscillatory signals toward the Oc1 and retrosplenial cortex (Yoshimura et al., 2003, 2005, 2007, 2016). Focusing on the area between Oc1 and Oc2, the signal behaviors obtained by optical recording methods show that the later oscillatory signals back-propagate along the same pathways that the initial propagating signals travel. However, this was an observation of a population of neurons. It is difficult to understand how a single neuron contributes to these dynamics. In this regard, whether to-and-fro waves travel through the same neuron is an important issue. If a single neuron elicits to-and-fro waves, it is suggested that the neuron sends not only a feedforward signal but also a feedback signal.

Therefore, we investigated caffeine-assisted oscillations in detail. The initial trigger signal is mainly dependent on non-NMDA receptor activity, and later back propagation is dependent on NMDA receptor activity. In our report in 2001, we showed waveforms of caffeine-assisted oscillations obtained from intracellular recordings (Yoshimura et al., 2001). The recordings were performed from layer II/III on Oc1 of rat brain slices. Oscillatory waves are composed of initially propagating waves and later back-propagating waves (Yoshimura et al., 2003). It is important to note that a single neuron has both an initial propagating wave and later back-propagating waves, showing that the to-and-fro signal behavior uses the same neuron. An individual neuron in layer II/III sends a non-NMDA receptor-dependent initial output and receives repetitive NMDA receptor-dependent inputs. Thus, it is presumed that these neurons may have excitatory axon collaterals. Previous anatomical studies confirm our findings. Feedback pathways from the extrastriate lateromedial visual area provide input directly to neurons in the primary visual cortex, which creates a reciprocal forward connection (Johnson and Burkhalter, 1997).

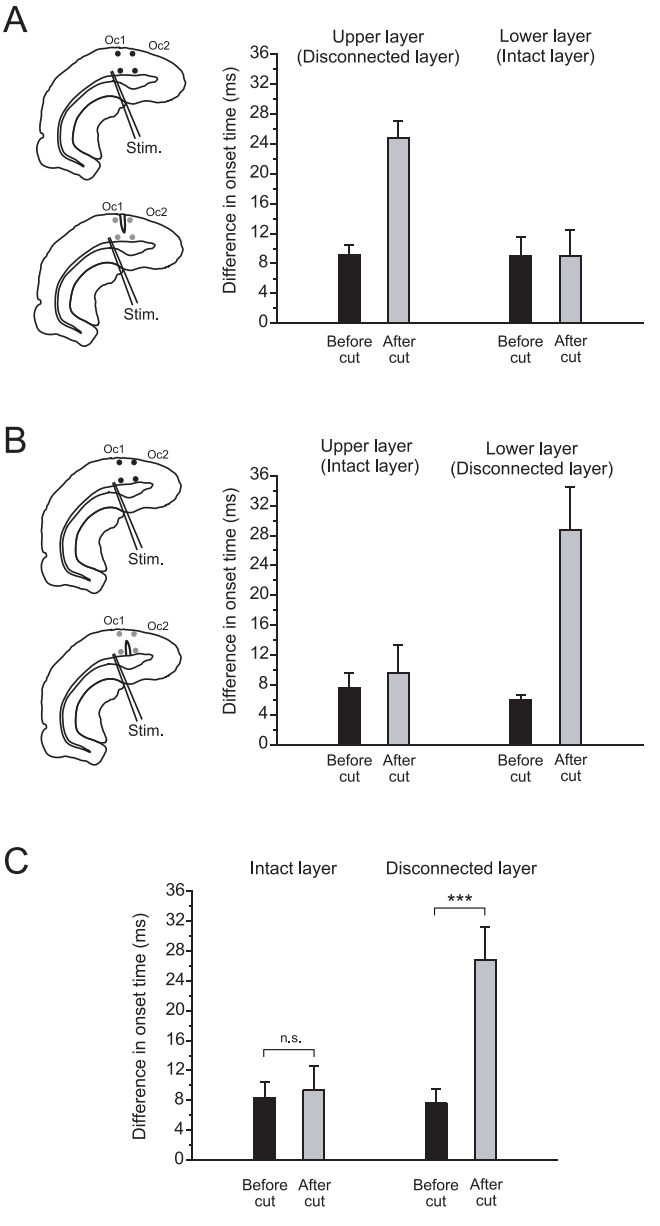

(caption on next column)

Fig. 4. Influences of the disconnection on onset time of oscillatory events. Illustration of slices indicating electrical stimulation sites, vertical cut sites, and ROIs. The ROIs were located at the upper-layer of the Oc1, upper-layer of Oc2M, the deep layer of Oc1, and the deep layer of Oc2M. Small black circles indicate locations where data were acquired before the slice cut, and small gray circles indicate locations where data were acquired after the slice cut. The data at the respective ROIs were acquired using optical recordings. In the graphs, black bar charts plot the differences in the onset times of oscillatory events generated at the medial and lateral ROIs before the slice cut. Similarly, gray bar charts plot the differences in the onset times of the oscillatory events at the two ROIs after slice cut. (A) Before and after the upper layer was cut. Left side of the graph: Comparison of differences in the onset time at two ROIs in the upper layer before and after slice cut (n = 3). Right side of the graph: Comparison of differences in the onset time at two ROIs in the lower layer before and after slice cut (n = 3). Note that the disconnection of the upper layer is likely to delay the onset times of the oscillatory events generated in the upper layer of Oc2M. (B) Cases before and after the lower layer cut. Left side of the graph: Comparison of differences in the onset time at two ROIs in the upper layer before and after slice cut (n = 3). Right side of the graph: Comparison of differences in the onset time at two ROIs in the lower layer before and after slice cut (n = 3). Note that the disconnection of the lower layer is likely to delay the onset times of the oscillatory events generated in the deep layer of Oc2M. (C) In the cases before and after partial vertical-layer cutting, together with results in (A) and (B). Left side in the graph: Comparison of the onset time differences along the intact layer before and after slice cutting (n = 6). Right side of the graph: Comparison of differences in the onset time at two ROIs in the disconnected layer before and after slice cut (n = 6). Note that the disconnection of the partial vertical layer significantly delays the onset times of oscillatory events generated in the disconnected layer of the Oc2M. The asterisk denotes a significant difference (***: paired t-test, $P = 3.32 \times 10^{-7}$, n = 6), and n.s. denotes that there is no significant difference.

Recently, it was demonstrated that when distal dendrites receive synchronous and clustered inputs with NMDA receptor-dependent components, the dendrites perform highly nonlinear integration, with the result that neurons show maximum responsiveness to synaptic inputs (Xiumin, 2014). In our observations, the optical responses as well as the local field potential are marked along layer II/III. This might indicate that distal dendrites receive synchronous and clustered inputs abundantly in layer II/III. This process may contribute to the establishment of interregional coupling.

4.2. Initial wave propagation from the Oc1 to the Oc2M: feedforward direction

In the present study, the main question is how dynamics of the oscillations will be affected if the signal traveling pathways are disconnected. Optical images obtained from optical recording methods show that, after electrical stimulation, the initial feedforward signals propagated in the horizontal direction within the neocortex and switched on the oscillator in Oc2M. However, neither the upper nor the lower layer cut disrupted signal propagation and oscillation induction. This may provide valuable information. Plausible interruption may occur when

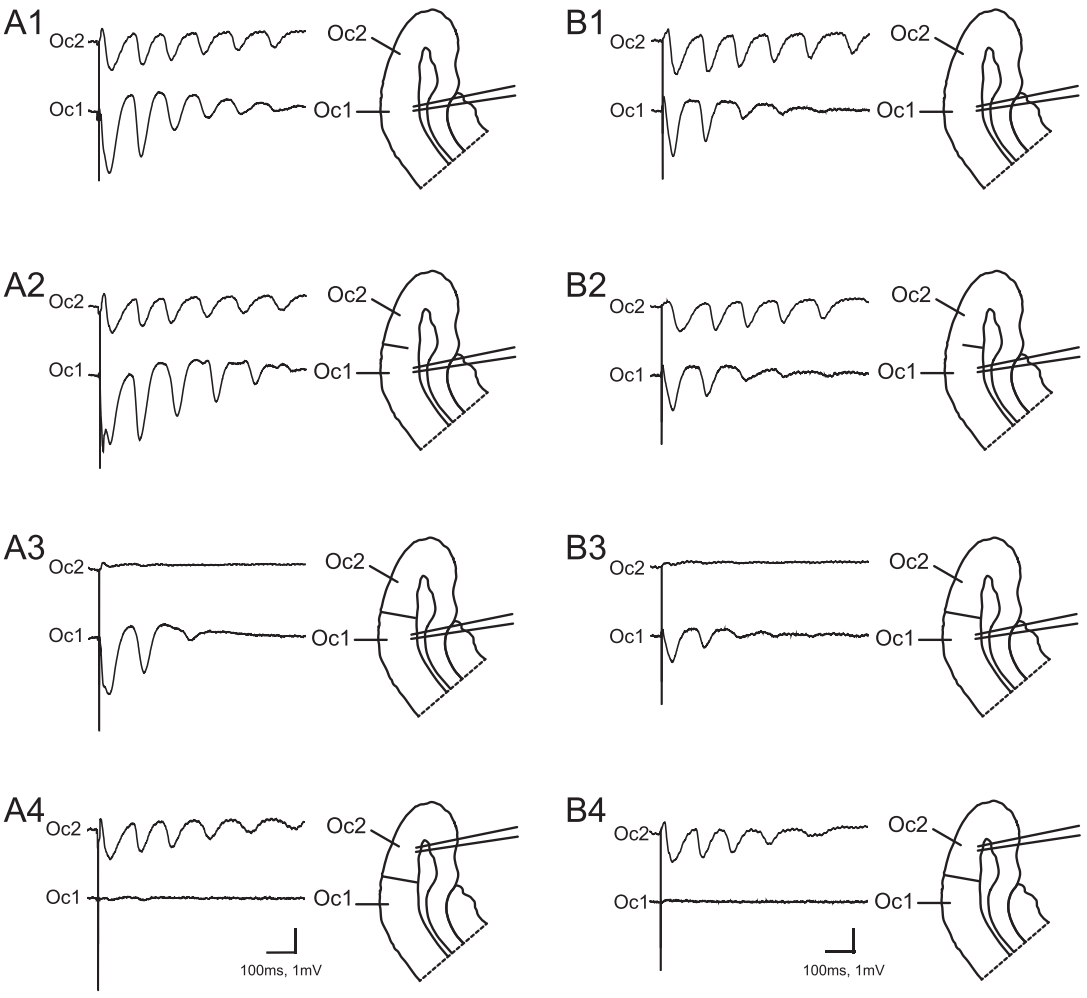

Fig. 5. Influences of disconnection at upper and/or lower layer on dynamics of oscillations. (A1–4) Simultaneous recordings of field potentials were obtained from Oc1 and Oc2M. The location of the stimulation electrode is shown in the line drawings. A1–4 were obtained from the same slices. A1: Simultaneous recordings were made from normal slices, and waveforms of the local field potential obtained from layers II/III are shown. Note that differences in the peak time of waves between the two traces indicate that the initial wave propagated from Oc1 to Oc2M, whereas later waves propagated from Oc2M to Oc1. A2: Simultaneous recordings were made from a slice of the upper-layer cut, and waveforms of the local field potential obtained from layers II/III are shown. Note that, similar to the case of a normal slice, differences in the peak time of waves between the two traces indicated that the initial wave propagated from Oc1 to Oc2M, whereas later waves propagated from Oc2M to Oc1. A3: Simultaneous recordings were made from slices of whole-layer cut, and waveforms of the local field potential obtained from layer II/III are shown. Note that stimulation of Oc1 did not generate oscillations in Oc2M. A4: Simultaneous recordings were made from slices of whole-layer cut, and waveforms of local field potential obtained from layers II/III are shown. Note that the stimulation of Oc2 did not generate oscillations in Oc1. (B1–4) Simultaneous recordings of field potentials were obtained from Oc1 and Oc2M. The location of the stimulation electrode is shown in the line drawings. B1–4 were obtained from the same slice. B1: Simultaneous recordings were made from normal slices, and waveforms of the local field potential obtained from layers II/III are shown. Note that differences in the peak time of waves between the two traces indicate that the initial wave propagated from Oc1 to Oc2M, whereas later waves propagated from Oc2M to Oc1. B2: Simultaneous recordings were made from the slice of the lower-layer cut, and waveforms of the local field potential obtained from layer II/III are shown. Note that, similar to the case of a normal slice, differences in the peak time of waves between the two traces indicated that the initial wave propagated from Oc1 to Oc2M, whereas later waves propagated from Oc2M to Oc1. B3: Simultaneous recordings were made from slices of whole-layer cut, and waveforms of local field potential obtained from layers II/III are shown. Note that stimulation of Oc1 did not generate oscillations in Oc2M. B4: Simultaneous recordings were made from slices of whole-layer cut, and waveforms of local field potential obtained from layer II/III are shown. Note that the stimulation of Oc2 did not generate oscillations in Oc1.

the upper and lower horizontal pathways are complementary when the signal travels within the neocortex.

When the upper pathway is disconnected, the signals travel toward the destination via the lower pathway. In contrast, when the lower pathway is disconnected, the signals travel toward the destination via the upper pathway. In the vertical pathway, when the upper pathway is disconnected, signals that pass through the deep pathway beneath the area of the disconnection travel from the deep to the upper area on the side of Oc2M. The signal then restarts along the upper layer. Thus, it takes time for the signal to start traveling along the upper layer (Figs. 2B, 4B). Meanwhile, however, the feedforward signal by way of a deep pathway continues traveling toward the destination. In layer VI, there are different classes of pyramidal neurons, such as cortical thalamic and corticocortical neurons. Layer VI corticocortical neurons have horizontally oriented axons that remain confined to deep layers, and their branches project to the secondary areas (Thomson, 2010). Thus, layer VI played an important role. In Fig. 2C, the initial wave at ROI 7 appears faster than the initial wave at ROI 6, indicating that the generation of waves at ROI 7 is triggered by the signal traveling along the deep pathway. These findings suggest that the vertical pathway also

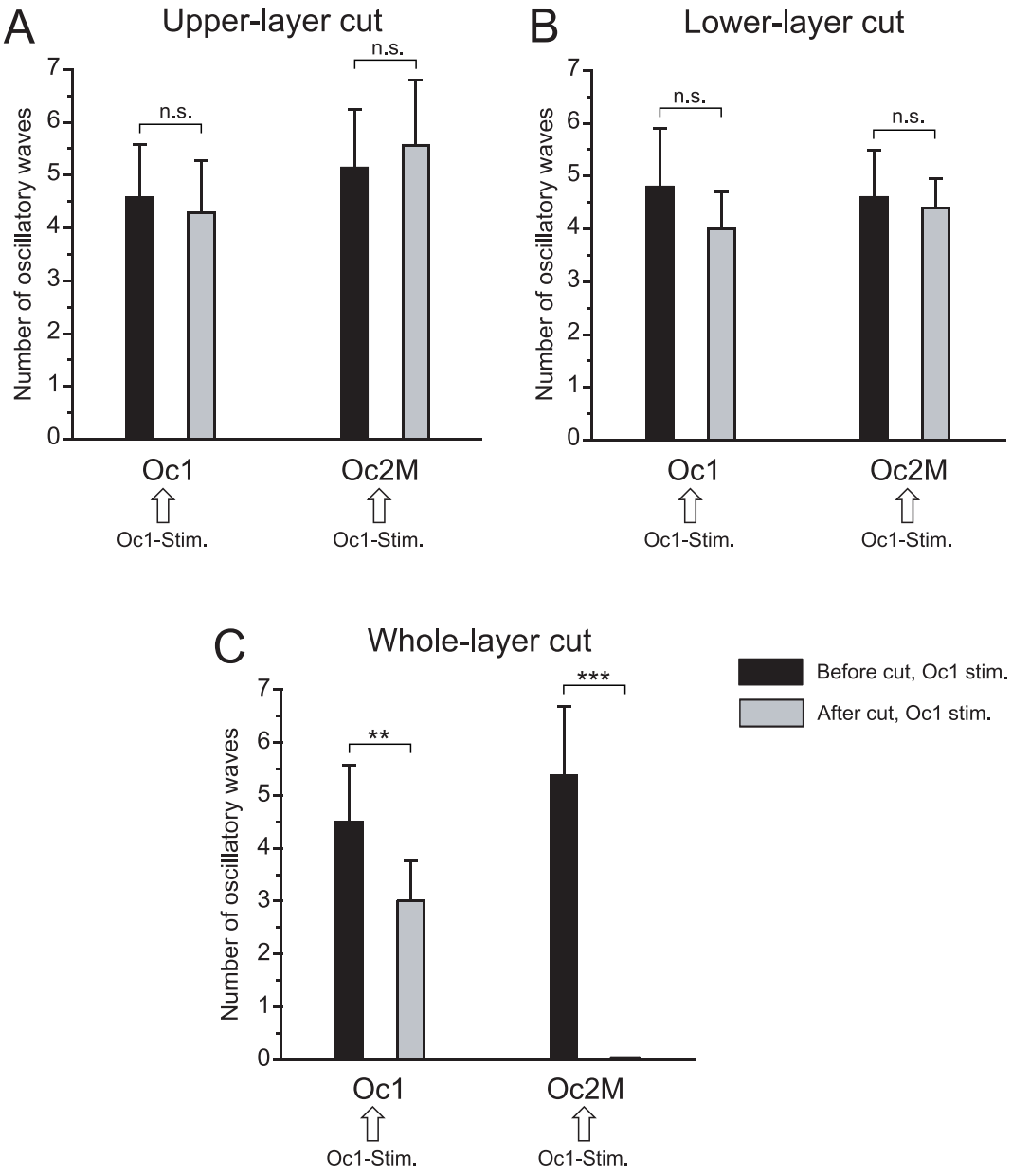

Fig. 6. Comparison of oscillation sizes before and after disconnection between Oc1 and Oc2M. Black bar charts plot averaged numbers of oscillation waves before slice cutting in the case of Oc1 stimulation. Light gray bar charts plot the averaged numbers of oscillation waves after slice cut in the case of Oc1 stimulation. In all cases, pairs of wavenumbers before and after disconnection were collected from the same slice. (A) Upper-layer cut: data were collected from Oc1 (n = 14) and Oc2M (n = 14); (B) Lower-layer cut: data were collected from Oc1 (n = 5) and Oc2M (n = 5); (C) Whole-layer cut: data were collected from Oc1 (n = 8) and Oc2M (n = 8). Pairs of waves collected in Oc1 and Oc2M are indicated, and a paired t-test is executed for every pair of cases. Note that in the case of the whole-layer cut, the oscillation size in Oc1 is attenuated. The asterisk denotes a significant difference (**: paired t-test, P = 0.0094, n = 8, ***: paired t-test, $P = 5.16 \times 10^{-7}$, n = 8), and n.s. denotes that there is no significant difference.

contributes to the signal traveling along the upper layer in Oc2M.

When the lower pathway is disconnected, signals that go through the upper area of the disconnection travel from the upper to the lower area on the side of Oc2M. Thus, it takes time for the signal to start traveling along the lower layer (Figs. 3B, 4B). Meanwhile, however, feedforward signals by way of the upper pathway continue traveling toward the destination. The difference between the case of the upper and lower layer cuts is that the initial signal propagation and generation of the oscillation along the upper horizontal pathway seemed not to be affected by the lower layer cut, but not the upper layer cut. Together with these findings, in both cases, the contribution of the upper and lower pathways for the initial signal propagation toward the horizontal direction may be an alternative by using a vertical pathway, as needed.

The same kinds of signal propagation in the visual cortex have been reported using optical recording with a voltage-sensitive dye. Tanifuji et al. demonstrated that, under the condition of disinhibition by applying 1 μM BMI to visual cortex slices, electrical stimulation to the white matter elicits vertical and horizontal signal propagation, which is similar to the initial phase of the present caffeine-assisted oscillations, and the effects of vertical upper and layer cuts were investigated. Under these conditions, signal propagation was maintained by avoiding a vertical cut, in which the signal propagated along the vertical connections (Tanifuji et al., 1994). This is similar to the initial phase of caffeine-assisted oscillations. Thus, in both cases, reciprocal vertical pathways worked together with horizontal pathways to establish stable signal communication.

4.3. Later backpropagation of oscillatory waves from the Oc2M to Oc1: feedback direction

When the horizontal lower pathway was disconnected, the back propagation of oscillatory signals from Oc2M to Oc1 was not affected (Fig. 3B), showing that the lower pathway was not necessary for back-propagation of oscillatory waves when the upper pathway was intact. This was also confirmed by the results of the simultaneous field potential recordings, presented in Fig. 5B1-B4. However, when the upper pathway is disconnected, it is difficult to interpret whether the lower pathway is required for the backpropagation of oscillatory waves from Oc2M to Oc1. The delay in entering the Oc2M of the initial trigger signal caused by the upper layer cut reflects a delay in the onset of the oscillation (Figs. 2B, 4A), showing that the oscillator in the Oc2M works independently, and later oscillatory waves do not seem to propagate from Oc2M to Oc1 in this case. We previously reported that the oscillation generator is also equipped with the lateral Oc2L (Yoshimura et al., 2005). When an oscillator exists in Oc2M and Oc2L simultaneously, oscillation may be generated independently when the initial signal switches on both oscillators (Yoshimura et al., 2005a, 2005b). However, in Fig. 5A1-A4, the back propagation of the later oscillatory waves may be dependent on the oscillator in Oc2M. In this case, the oscillator in Oc2L may not have been equipped. These observations suggest that the lower pathway contributes to the backpropagation of later oscillatory waves as needed when the upper layer is disconnected. In other words, when the oscillator exists in Oc2M only, oscillatory waves later propagate through the lower pathway, whereas when the oscillator exists both in Oc2M and Oc2L, the trigger signal drives the respective oscillator independently.

Regardless of the oscillator in Oc2L, backpropagation from Oc2M to Oc1 may have contributed to oscillatory events in Oc1. The reasons for this are as follows: An important finding of the present study is that the size of the oscillation in Oc1 is attenuated after the whole-layer cut between Oc1 and Oc2M (Figs. 5A3, 5 B3, 6C), suggesting that oscillatory events in Oc1 are assisted by the oscillator equipped in Oc2M. Therefore, the backpropagation by way of the intact layer must play an important role. Once the signal passes through an intact pathway, oscillation is generated using a vertical pathway. Thus, the contribution of the upper and lower pathways for later signal backpropagation may be an alternative by using horizontal and vertical pathways, as needed. This strategy may be owing to the fact that feedback connections are polysynaptic (Johnson and Burkhalter, 1997).

4.4. Oscillation generator

In general, synchronized oscillations are established in excitatory and inhibitory networks, in which the balance of excitation between recurrent and inhibitory networks influences the patterns of oscillations (Shu et al., 2003; Melamed et al., 2008; Sase et al., 2017; Singer, 2018; Lourenço et al., 2020; Zhang and Zhang, 2020). In the case of caffeine-assisted oscillations, the excitability of the excitatory network increases, during which caffeine acts on both excitatory and inhibitory neurons (Fredholm et al., 1999; Yoshimura et al., 2005a, 2005b). As the gain (E/I ratio) increases, an appropriate network for oscillation generation may emerge. For inhibitory networks, it is difficult to detect the voltage responses of inhibitory neurons by field potential recordings because the electrical fields produced by inhibitory neurons are symmetrical. Therefore, the source of the oscillation generator may be predicted from waveforms because the voltage responses produced by inhibitory neurons may be excluded. Considering electrical fields, field potential recordings can detect the relative strength of the current sink or flow at the recording site based on waveforms. In this study, we recorded the local field potentials in the upper and lower layers. The important finding is that the direction of the wave fluctuation was reversed between the oscillatory waveforms in the upper and lower layers. In addition, the direction of wave fluctuation was the same between the two recording sites in the horizontal upper layer (not shown here, see Yoshimura et al., 2003). These observations suggest that the source of oscillation does not exist between the horizontal layer II/III, but exists in vertical networks between the upper and lower layers. In other words, the oscillation generator was created from the network loop in the vertical direction. Thus, the column itself in Oc2M may be a candidate oscillator.

Optical recording methods using voltage-sensitive dyes can detect membrane potential depolarization, excitation strength, and neural activity dynamics. The excitatory strength is much higher in layer II/III than in the lower layer, showing that the current sink is prominent in layer II/III. However, the oscillator itself may not be localized within layer II/III, as mentioned above. Together with these considerations, the oscillation generator may be composed of a loop of vertical connections in the Oc2M, whereas the role of synaptic activities in layer II/III may be boosted by synchronized oscillation.

During one course of oscillation, the early oscillatory phase gradually shifts to the later oscillatory phase, in which the non-NMDA receptor-dominant phase shifts to the NMDA receptor-dominant phase (Yoshimura et al., 2016). This shift may be induced by repetitive synaptic activity within the upper layer of the recurrent network. Positive feedback via recurrent collateral connections can sustain persistent firing, and this kind of network is called the ‘attractor network’ (Rolls, 2010). Recently, it was proposed that recurrent networks in both the upper and lower layers of the neocortex form an ‘attractor network’. This idea is based on integrate-and-fire neural network simulations (Rolls and Mills, 2017). Limit cycle attractor is a case of the attractor networks, and the limit cycle attractor generate synchronized oscillation (Oku and Aihara, 2010; Thivierge et al., 2014). Changes in E/I balance can dramatically regulate the temporal rhythms of neural oscillations (Zhang and Zhang, 2020). According to the ‘neural mass model’, limit cycle attractors can generate alpha-like activity (Jin et al., 2022), and in the condition of increased E/I ratio, the limit cycle attractor generates alpha or theta band activity (Stefanovski et al., 2019). In our experiments, the application of caffeine generated oscillations at a frequency of approximately 8 Hz (Yoshimura et al., 2001), and may increase the E/I ratio. In addition, the distal dendrites in layer II/III receive clustered and synchronous inputs (Xiumin, 2014). Therefore, this may be an adequate condition for forming the limit cycle attractor in the upper layer of Oc2M. However, deep cortical neurons also have recurrent networks and the ability to form an attractor network that is connected to the upper layer networks. Considering this comprehensively, a neural oscillator might be composed of attractor networks in the upper and lower layers, in which the role of the upper layer is to boost oscillatory activities. In addition, the starting switch of the oscillator may be located at any point of the vertical loop because the oscillator is switched on by the signal from the upper layer as well as from the lower layers.

5. Conclusion

In the case of caffeine-assisted oscillations, interregional coupling is accomplished by signals traveling through the upper horizontal, lower horizontal, and vertical pathways. These pathways have the ability to convey oscillatory signals and function alternatively, even when the upper or lower pathway is disconnected. Neocortical horizontal and vertical connections might play a role as safety devices for interregional signal communication. In addition, together with our previous studies, it is suggested that the oscillation generator may be composed of a neural loop between the upper and lower layers, and that the upper layer may play a role as a booster of synchronized oscillations.

Ethics approval

All procedures performed in studies were in accordance with the National Institute of Health Guide for Care and Use of Laboratory Animals and its later amendments or comparable ethical standards. The institutional ethics committee at Kanazawa Medical University

(2012077) and Tokushima Bunri University (KP22–83–4) approved the present study.

CRediT authorship contribution statement

All authors contributed to the study conception and design. All experimental procedures were supervised and conducted by Hiroshi Yoshimura. Data collections were performed by Takako Fukuda, Hiroshi Yoshimura, Hiroyuki Kanayama and Takashi Tominaga. Material preparation was performed by Yoko Tominaga. Data analysis were performed by Takako Fukuda, Hiroshi Yoshimura and Nobuo Kato. All authors read and approved the manuscript.

Funding

This study was partly supported by grants from the Japan Society for that Promotion of Science (Grant Numbers 16K21734, 16H06532 and 21H03606 to TT), and was partly supported by grants from the Ministry of Education, Culture, Sports, Science and Technology of Japan (Grants-in-Aid for Scientific Research C22590966 to HY), and was partly supported by Research Clusters Program of Tokushima University, and Tokushima University President's Discretionary Fund.

Declaration of Competing Interest

The authors have no relevant financial or non-financial interests to disclose.

Data availability

Data will be made available on request.

Acknowledgments

None.

Informed consent

Not applicable.

References

Bressler, S.L., Menon, V., 2010. Large-scale brain networks in cognition: emerging methods and principles. Trends Cogn. Sci. 14, 277–290.
Buzáki, G., Draguhm, A., 2004. Neural oscillation in cortical networks. Science 304, 1926–1929.
Buzáki, G., Watson, B.O., 2012. Brain rhythms and neural syntax: implications for efficient coding of cognitive content and neuropsychiatric disease. Dialog. Clin. Neurosci. 14, 345–367.
Buzáki, G., Logothetis, N., Singer, W., 2013. Scaling brain size, keeping timing: Evolutionary presentation of brain rhythms. Neuron 80, 751–764.
Chadwick, A., van Rossum, M.C.W., Nolan, M.F., 2015. Independent theta phase coding accounts for CA1 population sequences and enables flexible remapping. eLife 4, e03542.
D'Souza, R.D., Wang, Q., Ji, W., 2022. Meier A.M., Kenne H., Knoblauch K., Bukhalter A. Hierachical and nonhierarchical feature of the mouse visual cortical network. Nat. Commun. 13, 503.
Douglas, R.J., Martin, K.A.C., 2004. Neuronal circuits of the neocortex. Annu. Rev. Neurosci. 27, 419–451.
Engel, A.K., Fries, P., Singer, W., 2001. Dynamic predictions: Oscillations and synchrony in top-down processing. Nat. Rev. Neurosci. 2, 704–716.
Ermentrout, G.B., Kleinfeld, D., 2001. Traveling electrical waves in cortex: Insight from phase dynamics and speculation on a computational role. Neuron 29, 33–44.
Fredholm, B.B., Battig, K., Holmen, J., Nehlig, A., Zuvartau, E.E., 1999. Actions of caffeine in the brain with special reference to factors that contribute to its widespread use. Pharmacol. Rev. 51, 83–133.
Jin, X., Zhang, Z., Zhang, L., Li, L., Huang, G., 2022. Using a new phase-locked visual feedback protocol to affirm simpler models for alpha dynamics. J. Neurosci. Metho 368, 109473.
Johnson, R.R., Burkhalter, A., 1997. A polysynaptic feedback circuit in rat visual cortex. J. Neurosci. 17, 7129–7140.
Lourenço, J., De Stasi, A.,M., Deleuze, C., Bigot, M., Pazienti, A., Aguirre, A., Giugliano, M., Ostojic, S., Bacci, A., 2020. Modulation of coordinated activity across cortical layers by plasticity of inhibitory synapses. Cell Rep. 30, 630–641.
Masquelier, T., Hugues, E., Deco, G., Thorpe, S.J., 2009. Oscillations, phase-of-firing coding, and spike timing-dependent plasticity: an efficient learning scheme. J. Neurosci. 29, 13484–13493.
Melamed, O., Barak, O., Silberberg, G., Markram, H., Tsodyks, M., 2008. Slow oscillations in neural networks with facilitating synapses. J. Comput. Neurosci. 25, 308–316.
Oku, M., Aihara, K., 2010. Dynamical inter-region coupling in the brain: A meso-scopic model from a dynamical system viewpoint. Nonlinear theory and its applications. EICE 1, 79–88.
!"count(.//sb:host[1]//child::*//sb:date)" > Panzeri, S., Macke, J.H., Gross, J., Kayser, C., . Neural population coding: combining insights from microscopic and mass signals. Trends Cogn. Sci. 19, 162–172.
Paxinos, G., Watson, C., 1997. The Rat Brain in Stereotaxic Coordinates, 4th ed..,. Academic Press, San Diego.
Petersen, S., Sporns, O., 2015. Brain networks and cognitive architectures. Neuron 88, 201–219.
Qi, S., Gao, Q., Teng, Y., Xie, X., Sun, Y., Wu, J., 2018. Multiple frequency bands analysis of large scale intrinsic brain networks and its application in schizotypal personality disorder. Front Comp. Neurosci. 12. Article 64.
Rolls, E.T., 2010. Attractor networks. WIREs Cogn. Sci. 1, 119–134.
Rolls, E.T., Mills, W.P.C., 2017. Computation in the deep vs superficial layers of the cerebral cortex. Neurobiol. Learn. Mem. 145, 205–221.
Sase, T., Katori, Y., Komuro, M., Aihara, K., 2017. Bifurcation analysis on phase-amplitude cross-frequency coupling in neural networks with dynamic synapses. Front. Comp. Neurosci. 11, Article 18.
Sejnowski, T.J., Paulsen, O., 2006. Network oscillations: Emerging computational principles. J. Neurosci. 26, 1673–1676.
Shao, Z., Burkhalter, A., 1996. Difference balance of excitatory and inhibition in forward and feedback circuits of rat visual cortex. J. Neurosci. 16, 7353–7365.
Shu, Y., Hasenstaub, A., McComick, D.A., 2003. Turning on and off recurrent balanced cortical activity. Nature 423, 288–293.
Singer, W., 2018. Neural oscillations: unavoidable and useful? Europe. J. Neurosci. 48, 2389–2398.
Singer, W., 2021. Recurrent dynamics in the cerebral cortex: Integration of sensory evidence with stored knowledge. Proc. Nat. Acad. Sci. Usa. 118, e2101043118.
Sporns, O., Honey, C.J., Kötter, R., 2007. Identification and classification of hubs in brain networks. PloS One 2, e1049.
Stefanovski, L., Triebkorn, P., Spiegler, A., Diaz-Cortes, M.-A., Solodkin, A., Jirsa, V., McIntosh, A.R., Ritter, P., 2019. Linking molecular pathways and large-scale computational modeling to assess candidate disease mechanisms and pharmacodynamics in Alzheimer's disease. Front. Comp. Neurosci. 13, Article 54.
Suo, X., Ding, H., Li, X., Zhang, Y., Liang, M., Zhang, Y., Yu, C., Qin, W., 2021. Anatomical and functional coupling between the dorsal and ventral attention networks. NeuroImage 232, 117868.
Swanson, L.W., 1992. Brain Maps: Structure of the Rat Brain, 2nd ed..,. Elsevier,, Amsterdam.
Tanifuji, M., Sugiyama, T., Murase, K., 1994. Horizontal propagation of excitatory in rat visual cortical slices revealed by optical imaging. Science 266, 1057–1059.
Thivierge, J.-P., Comas, R., Longtin, A., 2014. Attractor dynamics in local neural networks. Front. Neural Circuits 8. Article 22.
Thomson, A.M., 2010. Neocortical layer 6, a review. Front. Neural Circuits 4. Article 13.
Tominaga, T., Tominaga, Y., Ichikawa, M., 2002. Optical imaging of long-lasting depolarization on burst stimulation in area CA1 of rat hippocampal slices. J. Neurophysiol. 88, 1523–1532.
Xiumin, L., 2014. Signal integration on the dendrites of a pyramidal neuron model. Cogn. Neurodyn 8, 81–85.
Yoshimura, H., 2005a. The potential of caffeine for functional modification from cortical synapses to neuron networks in the brain. Curr. Neuropharmacol. 3, 309–316.
Yoshimura, H., Sugai, T., Onoda, N., Segami, N., Kato, N., 2001. Synchronized population oscillation of excitatory synaptic potentials dependent of calcium-induced calcium release in rat neocortex. Brain Res 915, 94–100.
Yoshimura, H., Kato, N., Sugai, T., Segami, N., Onoda, N., 2003. Age-dependent enhancement of oscillatory signal flow between the primary and secondary visual cortices in rat brain slices. Brain Res 990, 172–181.
Yoshimura, H., Sugai, T., Segami, N., Onoda, N., 2005b. Strengthening of non-NMDA receptor-dependent horizontal pathways between primary and lateral secondary visual cortices after NMDA receptor-dependent oscillatory neural activities. Brain Res 1036, 60–69.
Yoshimura, H., Mashiyama, Y., Kaneyama, K., Nagao, T., Segami, N., 2007. Opening of shortcut circuits between visual and retrosplenial granular cortices of rats. NeuroReport 18, 1315–1318.
Yoshimura, H., Sugai, T., Kato, N., Tominaga, T., Tominaga, Y., Hasegawa, T., Yao, C., Akamatsu, T., 2016. Interplay between non-NMDA receptor activation during oscillatory wave propagation: Analyses of caffeine-induced oscillations in the visual cortex of rats. Neural Netw. 79, 141–149.
Young, H., Belbut, R., Baeta, M., Petreanu, 2021. L. Lamina-specific cortico-cortical loops in mouse visual cortex. eLife 10, e59551.
Zhang, Y., Zhang, X., 2020. Portrait of visual cortical circuits for generating neural oscillation dynamics. Cogn. Neurodyn. https://doi.org/10.1007/s11571-020-09623-4.
Zilles, K., Wree, A., 1995. Cortex. In: Paxinos, G. (Ed.), The Rat Nervous System, 2nd ed..,. Academic Press, Inc, San Diego, pp. 649–685.